

# We are IntechOpen, the world's leading publisher of Open Access books Built by scientists, for scientists

6,900

Open access books available

186,000

International authors and editors

200M

Downloads

Our authors are among the

154

Countries delivered to

TOP 1%

most cited scientists

12.2%

Contributors from top 500 universities



WEB OF SCIENCE™

Selection of our books indexed in the Book Citation Index  
in Web of Science™ Core Collection (BKCI)

Interested in publishing with us?  
Contact [book.department@intechopen.com](mailto:book.department@intechopen.com)

Numbers displayed above are based on latest data collected.  
For more information visit [www.intechopen.com](http://www.intechopen.com)



# An Assessment of the Conformational Profile of Neuromedin B Using Different Computational Sampling Procedures

Parul Sharma<sup>1</sup>, Parvesh Singh<sup>1</sup>, Krishna Bisetty<sup>1</sup> and Juan J Perez<sup>2</sup>

<sup>1</sup>Department of Chemistry, Durban University of Technology, Steve Biko campus, Durban

<sup>2</sup>Department d' Enginyeria Quimica, UPC, ETS d'Enginyers Industrials, Barcelona

<sup>1</sup>South Africa

<sup>2</sup>Spain

## 1. Introduction

Neuromedin B (NMB) (Minamino et al., 1983), a ten residue (GNLWATGHFM-NH<sub>2</sub>, Figure 1) neuropeptide, belongs to the ranatensin subfamily of bombesin-like peptides (Erspamer, 1980) which exhibits a wide range of biological responses in the central nervous system and gastrointestinal tract including thermoregulation (Marki et al., 1981), stimulation of the secretion of gastrointestinal hormones (Ghatei et al., 1982), regulation of smooth muscle contraction (Erspamer, 1988), the ability to function as a growth factor in small cell lung cancer cells and murine 3T3 cells (Corps et al., 1985; Cuttitta et al., 1985; Moody et al., 1985). Its mechanism of action involves the initial binding to the three cell surface receptors (Ohki-Hamazaki, 2000) with different pharmacological profile: the neuromedin B receptor (NMB-R or bb1) (Wada et al., 1991), the gastrin-releasing peptide receptor (GRP-R, or bb2) (Corjay et al., 1991), and bombesin receptor subtype 3 (BRS-3, or bb3) (Gorbulev et al., 1992). NMB binds to NMB-R with highest affinity, GRP-R with lower affinity and BRS-3 with lowest affinity (Mantey et al., 1997).

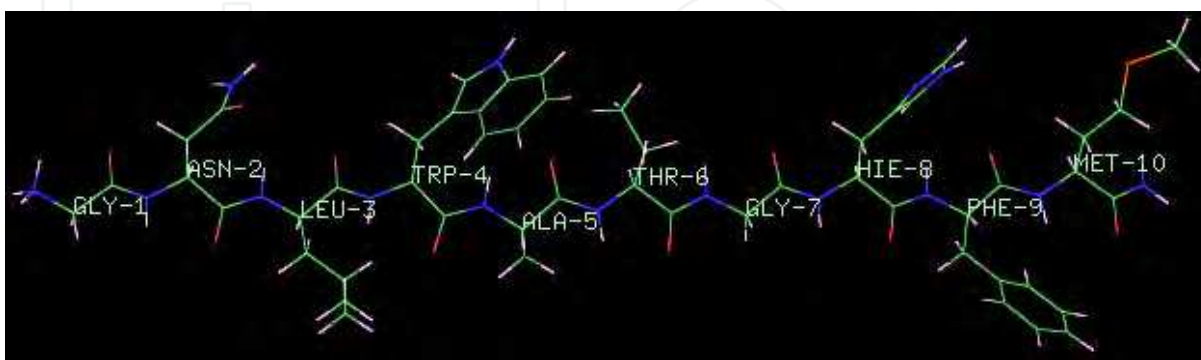


Fig. 1. Extended structure of Neuromedin B showing different residues

A number of spectroscopic studies of NMB including nuclear magnetic resonance (NMR) (Lee & Kim, 1999), Infrared (IR) (Erneand & schwyzer, 1987), Circular Dichroism (CD) and Fluorescence spectroscopy (Polverini et al., 1998) are widely reported in the literature. A

recent study of the structure activity relationship (SAR) of bombesin (Glp-Gln-Arg-Leu-Gly-Asn-Gln-Trp-Ala-Val-Gly-His-Leu-Met-NH<sub>2</sub>) using alanine scan to determine the contribution of specific residues to a protein's function by mutating the residues to alanine (Horwell et al., 1996), suggested that Trp<sup>4</sup>, His<sup>8</sup> and Leu<sup>12</sup> residues corresponding to Trp<sup>4</sup>, His<sup>8</sup> and Phe<sup>9</sup> respectively in NMB, are important for the binding to the NMB receptors (Sainz et al., 1998). It is reported that (Erneand & schwyzer, 1987) in the phospholipids bilayer NMB adopts  $\alpha$ -helical conformation in the C-terminal region. Recent studies have demonstrated that small peptides are able to exist in a dynamic equilibrium between folded and unfolded structures, depending on the solvent polarity and their interaction with the membrane phase (Erne et al., 1985). In aqueous solutions small peptides are known to adopt many conformations since the hydrogen bond formation between the polar backbone carbonyl and the amide groups and water solvent effectively competes with an intramolecular hydrogen-bond formation (Erne et al., 1985; Kaiser & Kezdy, 1987; Zhong & Jr. Johnson, 1992). Based on CD, fluorescence and molecular dynamics (MD) studies (Polverini et al., 1998), it has been observed that NMB adopts an  $\alpha$ -helical structure in an apolar environment. However, in aqueous solution NMB adopts unordered and very flexible structures. In vacuum 50% of the structures of NMB are helix-like, with a right-handed chirality beginning from the tryptophan residue through to the C terminus and was found to be independent of the initial conformation. Moreover, two-dimensional (2D) NMR studies of NMB suggest that the peptide adopts a relaxed helical conformation from Trp<sup>4</sup> to Met<sup>10</sup> in a 50% aqueous trifluoroethanol (TFE) solution, and in 150 mM sodium dodecyl sulfate (SDS) micelles. Several reports also suggested that there might be a conformational change to a  $\beta$ -turn type structure upon binding to the receptor (Coy et al., 1988; Rivier & Brown, 1978). Despite being remarkably vital, spectroscopic methods alone cannot provide all the structural details necessary to fully understand the conformational profile of the peptides in solution due to the flexibility of these molecules. Therefore, despite having a great biological and pathological significance, the unique native conformation of NMB has not yet been clearly elucidated on the basis of available spectroscopic results.

Computational studies on the other hand, can provide detailed complementary information about the intrinsic conformational features of the peptide. The methodologies available nowadays to investigate the propensities of a peptide to adopt different conformations are solid enough to provide a reasonable picture of the conformational features of a peptide and the way the solvent affects them. Recently, Generalized Born surface area implicit solvent models (Calimet et al., 2001; Dominy & Brooks, 1999) have been used in bimolecular simulations. This methodology has become popular, especially in molecular dynamics applications due to its relative simplicity and computational efficiency, compared to the more standard numerical solution of the Poisson-Boltzmann (PB) equation. The recent modifications to the standard GB implementations extend its applicability to the entire range from low- to high dielectric environments and thus play an imperative role to reproduce the environment induced by different explicit solvents (Feig & Brooks, 2004; Sigalov et al., 2005).

The present work involves the employment of different computational procedures to explore the configurational space of NMB and to provide an adequate atomic description of the peptide, compatible with the aggregated information provided by different experimental techniques. Specifically, the configurational space of NMB peptide has been explored using standard molecular dynamics (MD), multi-canonical replica exchange

molecular dynamics (REMD) and simulated annealing (SA) sampling techniques using the Langevin thermostat. The Onufriev, Bashford, and Case (OBC) implicit water model (Onufriev et al., 2004) has been employed for the current investigations as this solvent model in combination with AMBERff96 is reported to generate a better extent of the helices and  $\beta$ -sheet conformations in peptides (Terada & Shimizu, 2008).

## 2. Computational methods

### 2.1 Replica Exchange Molecular Dynamics (REMD)

The leap module of AMBER 9 (Case et al., 2006) was used to generate the extended conformation of NMB with its N-terminal protonated and C-terminal amidated. The extended structure of NMB was energetically minimized until a convergence criterion of  $0.005 \text{ kcal mol}^{-1} \text{ \AA}^{-1}$  was achieved. REMD was subsequently performed on the minimized structure using the Generalized Born implicit solvent model (solvent dielectric constant 78.5, surface tension  $0.005 \text{ cal/mol}^{-1} \text{ \AA}^2$ ) was used to model the effects of solvation (Sitkoff et al., Tsui & Case, 2001). The internal dielectric constant around the peptide was set to 1. The SHAKE algorithm with a relative geometric tolerance of  $10^{-5}$  was used to constrain all bond lengths to their equilibrium distances. Prior to the REMD simulations, standard MD simulations were performed for 5 ns at different temperatures ranging from 200 to 900 K, with a temperature difference of 100 K. In the present study, twelve replicas were used and the temperature of each replica was set to: 277, 300, 326, 354, 385, 419, 457, 498, 544, 595, 651, and 713 K, with a time step of 0.2 fs. The temperature during the MD simulations was regulated by the Langevin thermostat (Wu & Brooks, 2003; Andersen, 1980). Each replica was simulated simultaneously and independently at different replica temperatures. The replica exchange was performed every 2 ps for 50,000 steps during the REMD simulations.

### 2.2 Molecular Dynamics (MD)

MD trajectory was undertaken using the Generalized Born (GB) approximation at 300 K employing the Langevin coupling algorithm. Internal dielectric constant around the peptide was set to 1, while the external dielectric constant of 78.5 corresponding to water was employed. In order to mimic the physiological conditions a 0.2 M salt concentration was used. SHAKE was used on all bonds involving hydrogen atoms with a time-step of 2 fs.

### 2.3 Simulated Annealing (SA)

The extended conformation of NMB peptide was energy minimized using the steepest descent method followed by a conjugate gradient method until a convergence of less than  $0.001 \text{ kcal mol}^{-1} \text{ \AA}^{-1}$  between successive steps was achieved using the SANDER module of AMBER 9 (Case et al., 2006). The SA calculation was performed under implicit solvent conditions using the GB-OBC continuum solvent model (Onufriev et al., 2004). For this purpose, all electrostatic calculations throughout this study were done with the relative permittivity of 80. The minimized starting structure was heated up to 900 K at a rate of  $100 \text{ K ps}^{-1}$ . This means that the structure was first heated to 200 K, allowed to equilibrate and then reheated to 300 K, and this heating process was repeated until a temperature of 900 K was reached. The high temperature was used to provide the molecules with sufficient kinetic energy to enable them to cross energy barriers between different conformations, as quickly as possible. At this point the

structure was slowly cooled from 900 K down to 200 K at a rate of 50 K ps<sup>-1</sup>. In this technique the system was cooled down at regular time intervals, by decreasing the simulation temperature from 900 K to 200 K in intervals of 50 K. As the temperature approaches 200 K the molecule is trapped in the nearest local minimum conformation. At the end of the annealing cycle, the geometry of the structure was minimized at 200 K, in order to remove the internal strain of the molecule. Information regarding the coordinates and minimized energy data at 200 K is saved separately on a data file, which completes a single cycle of simulated annealing. Subsequently the optimized structure was used as the starting conformation for the next cycle of SA. The 8000 cycles of iterative simulated annealing resulted in a library of 8000 structures accumulated (with each cycle corresponding to a single structure), and ranked according to their energy values. The primary objective of a conformational analysis is in the identification of low energy structures, which forms an important part of understanding the relationship between the structure and the biological activity of a molecule. The biological activity of a drug molecule depends on a single unique conformation hidden amongst all the low energy conformations (Ghose et al., 1989). The search for this so-called bioactive conformation for sets of compounds is one of the major tasks in medicinal chemistry. Only the bioactive conformation can bind to the specific macromolecular environment at the active site of the receptor protein (Jørgensen, 1991). An understanding of the manipulation of the conformational structures of peptides using highly restricted segments ultimately leads to the design of bioactive peptides to fit the three dimensional receptor site requirements. In the identification of low energy structures, the SA strategy employed is widely used in the characterization of low energy conformations (Ghose et al., 1989), and the following protocols were used. Firstly, the structures were rank-ordered by energy every 100 cycles and checked for uniqueness. The efficiency of this process was monitored according to the equation 1:

$$\lambda(N) = \frac{\xi(N)100}{N\xi(100)} \quad (1)$$

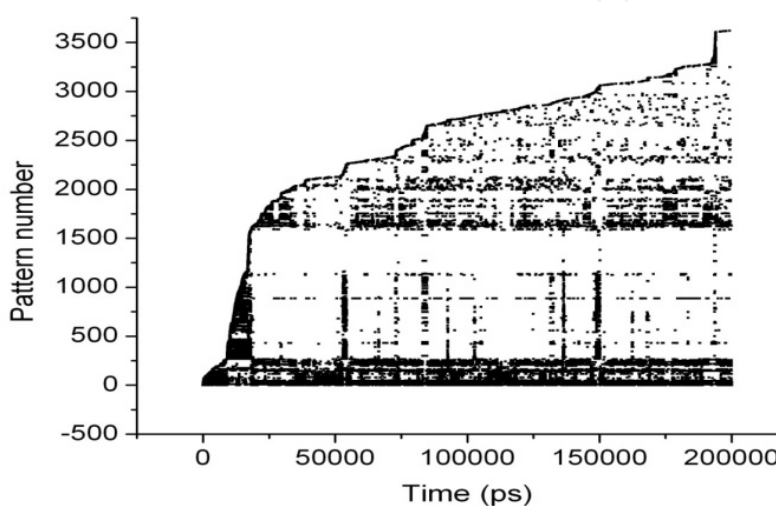
The efficiency parameter,  $\lambda$ , was computed every 100 cycles of SA, which is defined as the number of unique conformations,  $\xi$ , found after N cycles of SA,  $\xi(N)$ , divided by N, and adjusted by a coefficient so that the efficiency parameter is unity after the first 100 cycles performed, which completes the criterion of the iterative process (Corcho, 1999). The procedure was terminated in all cases when the calculated efficiency of the process,  $\gamma$  was at least 10% below the starting value. The evolution of this parameter was monitored along the conformational profile, for the peptide.

### 3. Results and discussion

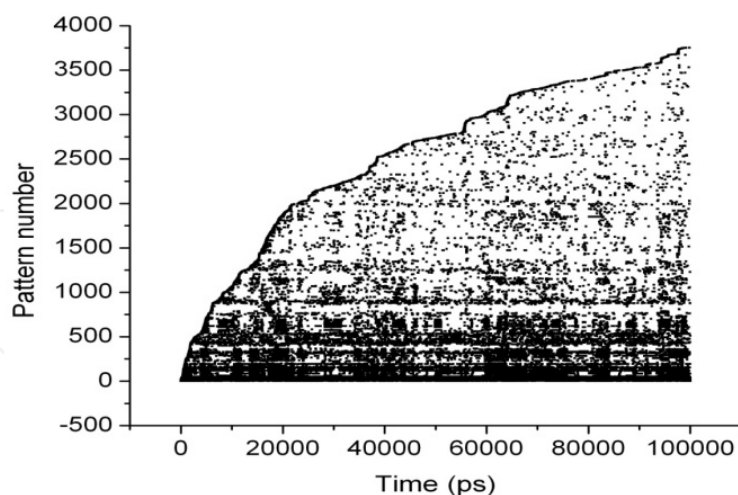
The sampling efficiency of MD and REMD trajectories was monitored by establishing different conformational patterns attained by NMB during the progress of the simulations. For this purpose, the CLASICO program (Corcho, 2004) was used to compute the pattern profile for every snapshot of MD and REMD trajectories, and is depicted in Figure 2a and Figure 2b, respectively. Accordingly, 105 439 (52.7%) patterns (Figure 2a) were obtained for 200 000 snapshots of MD whereas 68 753 (68.7%) patterns (Figure 2b) were identified for 100 000 snapshots of REMD trajectory. These plots provide a broad estimation of the performance of the different protocols in sampling new patterns. A closer inspection of Figure 2a reveals the appearance of new patterns in a uniform fashion for initial 10 ns trajectory probably due to



folding of the peptide. A sharp increase in patterns number was observed for the next 10 ns followed by a slow but regular increase of patterns throughout the trajectory. However, the peptide conformations seem to get trapped (dark areas) in regions of the conformational space at certain intervals clearly suggesting its restrictive nature to explore new patterns. In the case of REMD (Figure 2b), conformations with new patterns were sampled from the start of the simulation and progresses in a uniform fashion during the expansion of the trajectory. Moreover, the presence of less darker regions in the plot (Figure 2b) reveals that new patterns are explored with less restriction, clearly suggesting the better sampling performance of REMD over MD. Moreover, convergence seems to be attained in case of REMD after 100 ns as the appearance of new patterns was almost negligible at the end of trajectory.



(a)



(b)

Fig. 2. Evaluation of new patterns for the NMB in (a) MD and (b) REMD trajectories.

Secondary structure analysis was performed for every snapshot of MD and REMD calculations using the CLASICO program (Corcho, 2004) employing a three-residue window. Figures 3a-3b represents the statistics of the conformational motifs for each residue

of the NMB peptide in MD and REMD trajectories, respectively. Figure 3a shows the classification of secondary structures obtained in MD trajectory where the peptide exhibits predominantly  $\beta$ -turns (~25%) between residues 3 to 9 residues with a stronger propensity between residues 5 and 6. Additionally, an  $\alpha$ -helical region (4-5%) flanked by residues 3 to 6 was also observed in some of the sampled structures (Figure 3a) with the complete absence of  $3_{10}$ -helical conformations.

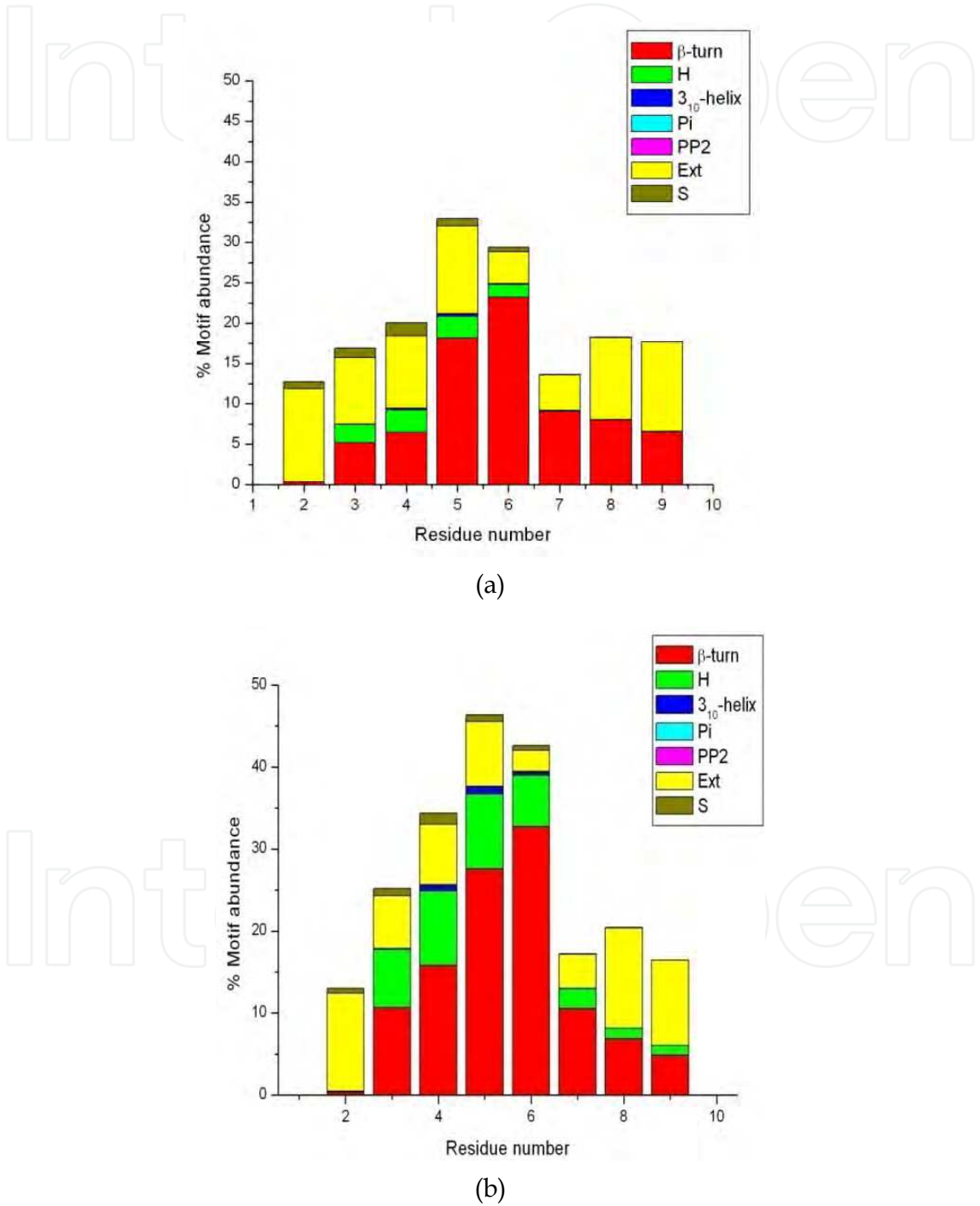


Fig. 3. Motif abundance for NMB in (a) MD and (b) REMD trajectories. Conformational motifs are labeled: H ( $\alpha$ -helix), PI ( $\pi$ -helix), PP2 (polyproline II), Ext (extended), S ( $\beta$ -strand).

To some extent  $\beta$ -strands (2-3%) in a region between residues 2 to 6 were also found in some of the conformations. The REMD protocol (Figure 3b) on other hand, was more efficient at inducing  $\beta$ -turns (~33%) in the sampled conformations flanked by residues 2 to 9 with a strong propensity between residues 5 and 6. The second major conformational motif attained by sampled structures in the REMD trajectory was  $\alpha$ -helical region (8-10%) flanked by residues 3 to 9 with a good propensity between residues 3 to 6 whereas a very low propensity between residues 7 to 9. All  $\alpha$ -helical conformations were observed to be right-handed, and to a minor extent conformations exhibiting  $3_{10}$ -helical region between residues 4 to 6 were also obtained (Figure 3b). Structures with  $\beta$ -strands between residues 2 to 6 were also observed in REMD calculations.

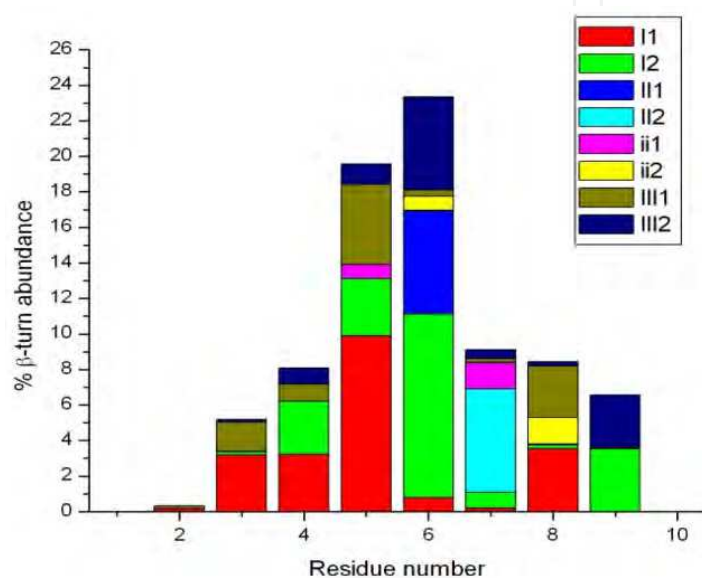
The  $\beta$ -turn motifs attained by residues of the NMB peptide were further classified into different types using two-residue window of the CLASICO program (Corcho, 2004), and are depicted in the Figures 4a-4b. The motifs obtained in MD trajectory (Figure 4a), shows the predominance of  $\beta$ -turn type I between residues 4 and 9 with a high propensity of type II between residues 6 and 7. To some extent  $\beta$ -turn type III was also observed between residues 3 to 9, with a high propensity between residues 5 and 6 and a low propensity between residues 3 to 4 and 7 to 9. In addition,  $\beta$ -turn type ii (mirror conformation of  $\beta$ -turn type II) was also observed between residues 5 to 8 (Figure 4a). On the other hand, conformations obtained from the REMD trajectory attain preferably  $\beta$ -turn type I between residues 3 to 9 with a strong propensity between residues 3 to 6 (Figure 4b). Structures displaying  $\beta$ -turn type III flanked by residues 3 to 9, with a strong propensity between residues 5 and 6 were also sampled in REMD trajectory. It should be noted that the CLASICO program does not include the first and last residues of the peptide in the secondary structure calculations which accounts for the absence of any of secondary structural features in Figures 3-4.

Since, the computational analysis described above provides an estimation of the average structure of NMB, it was considered worthwhile to compare the results of the different protocols with the reported NMR experiments reported in literature (Lee & Kim, 1999). The average distances corresponding to NMR NOE's were computed independently using the Clasterit algorithm of the CLASICO program (Corcho, 2004). Distances are reported as the average of the distance computed for each snapshot with a tolerance factor of  $\pm 1.96$  standard deviations, covering a 95% of the variance assuming that they exhibit a normal distribution. In case of long distances (LD), the NOEs considered in the present study include: i)  $C\beta$ -N (bN2) between residues 2-4(m), 4-6 (w), 5-7(w) and 6-8 (w); ii)  $C\alpha$ -N (aN3) between residues 4-7(m), 5-8(w), 6-9(m), and 7-10(m); iii)  $C\alpha$ -N (aN2) between residues 1-3(w), 2-4(m), 4-6(m), 5-7(w), 6-8(m), 7-9(w), 8-10(w), and 9-N(w) [14]. In case of short distances (SD), the NOEs include: i)  $C\alpha$ -N (aN1) between residues 1-2(s), 2-3(s) and 7-8(s); ii) N-N (NN1) between residues 2-3(w), 3-4(s), 6-7(s), 7-8(s), 8-9(s), 9-10(s), 10-N(w). In both cases, m, w and s stand for medium, weak and strong NOEs respectively.

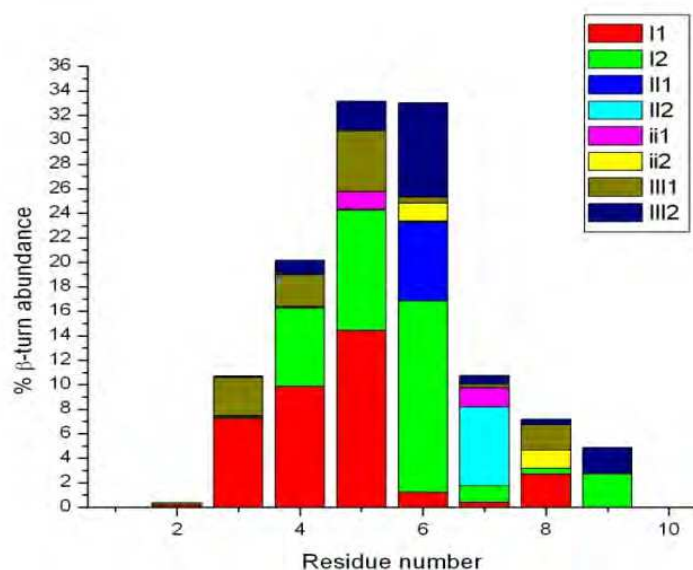
The overlaps between distances obtained from NMR experiments and those computed from the present studies are depicted in Figures 5a-d. These overlapping results compare both long distances (i to i+2 and i to i+ 3 type interactions) and short distances (i to i+1 type interactions) between the atoms. Specifically, Figure 5a reveals that only 12 long distances (LD) in the case of MD are in agreement with the corresponding NMR distances, and clearly suggests the absence of NMR structure in this simulation. Since, only LD accounts for the secondary



structures, a good agreement of short distances (SD) in case of MD (Figure 5c) does not make any contribution in the helicity. On the other hand, all computed LD (Figure 5b) and SD (Figure 5d) from REMD calculations corresponds to the NMR distances, clearly revealing the presence of the NMR structure. However, elongation of the computed distances (Figures 5b and 5d) clearly reveals the rapid exchange between NMR and unordered structures in this segment of trajectory. Overall these results reveal that peptide is in a rapid equilibrium between ordered and unordered conformations and suggests low conformational energy barrier between them accounting for the higher flexibility of NMB. Moreover, REMD method is more efficient to induce helicity and  $\beta$ -turns in the peptide and was also successful in sampling the NMR structures which were completely absent in the MD trajectory.



(a)



(b)

Fig. 4. Type of  $\beta$ -turns attained by NMB peptide in (a) MD and (b) REMD trajectories.

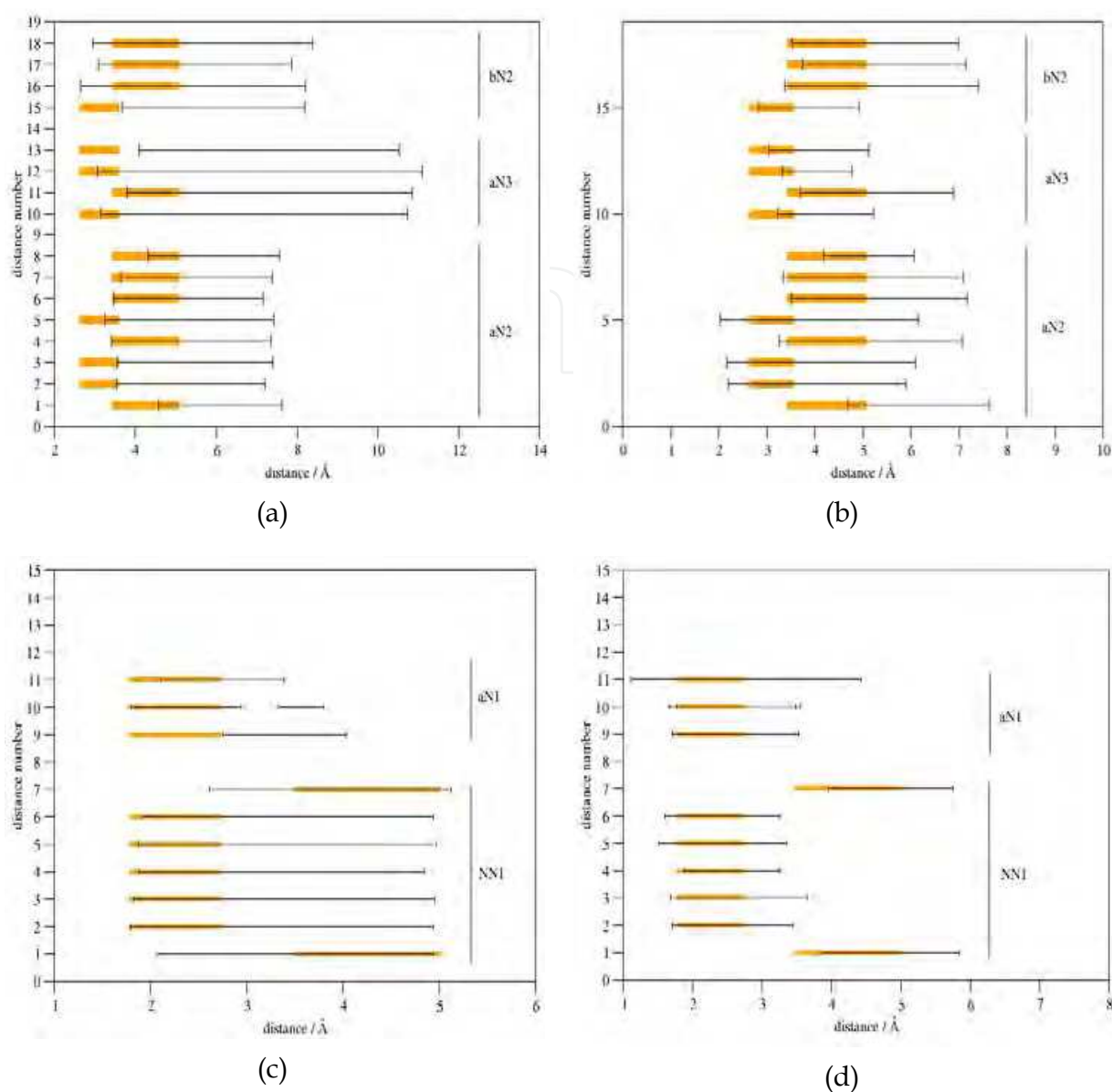


Fig. 5. Comparison of NMR derived long distances (LD) obtained from Lee & Kim, 1999 shown in orange and the computed average distances in a interval containing 95% of the structures for **(a)** MD and **(b)** REMD trajectories. Similar comparison of short distances (SD) for **(c)** MD and **(d)** REMD trajectories.

The conformational searches for NMB presented in this study were performed with the simulated annealing (SA) protocol in an iterative fashion, as a sampling technique. The sampling procedure was stopped after 8000 cycles of an iterative SA process for which the sampling efficiency  $\lambda$  (see Eqn. 1) was found to be less than 10% of the starting value. The evolution of this parameter  $\lambda$  was computed using Eqn. 1 and monitored along the conformational profile, as shown in Figure 6.

The shape of the above figure suggests that the search procedure employed was acceptable both in quality and computer time. Low levels of performance were reached in finding new low energy conformations ( $\lambda = 0.1$ ) which is the expected result for most peptide analogues

(Filizola et al., 1998). After completion of 8000 cycles of SA, the resulting 8000 structures were stored in a library. The criterion described in the Methods Section 2.3 was used to compute the total number of unique conformations for the NMB peptide. Of the total 5521 unique conformations, only 205 low energy structures ( $<5$  kcal mol<sup>-1</sup>) were observed (Table 1).

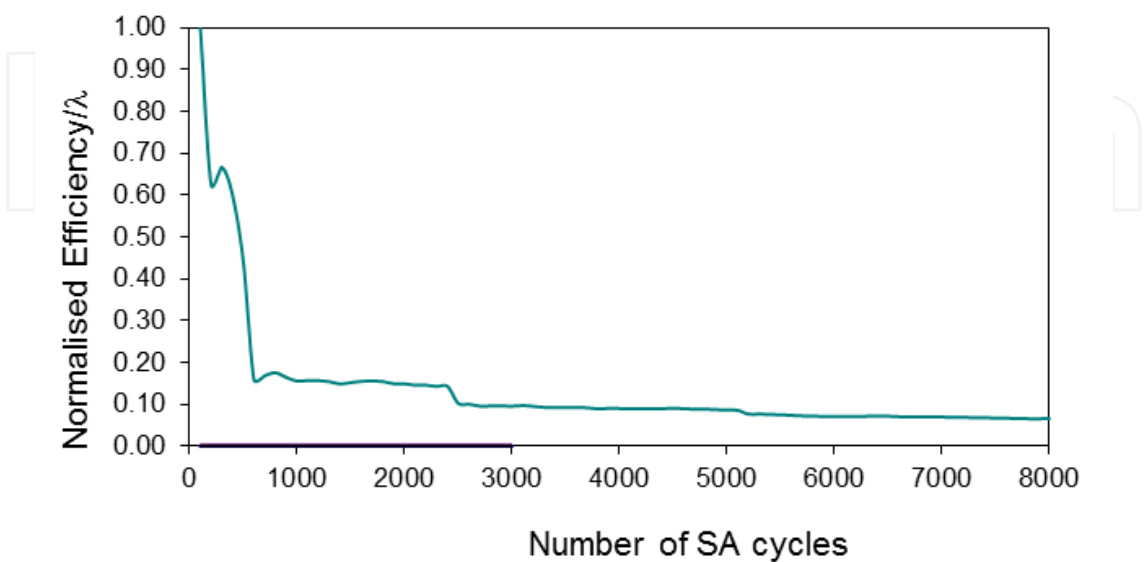


Fig. 6. Normalised efficiency values for the NMB peptide search.

NMB sequence	Total number of unique conformations	Number of classes obtained from cluster analysis	Number of unique conformations within 5 kcal mol <sup>-1</sup>
H-GNLWATGHFM-NH <sub>2</sub>	5521	10	205

Table 1. Summary of conformational analysis obtained from SA

To describe the preferred conformational domains exhibited by the peptide, the low energy structures were clustered into groups according to the values of the root mean square deviation (RMSD) of the distances between the backbone atoms of every structure.

Furthermore the RMSD's for the unique conformations were calculated using the Kleiweg clustering method (Kleiweg et al., 2004) to perform the hierarchical cluster analysis. The clustering can be visually represented by constructing a dendrogram, which indicates the relationship between the items in the data set (i.e. RMSD) and is graphically represented in Figure 7. The dendrogram enables us to identify how many clusters there are at any stage and what the corresponding members of the clusters are. It is a useful tool to show the underlying structure of the data and for suggesting the appropriate number of clusters to choose. A line drawn horizontally across the dendrogram enables one to read off how many clusters there are at any particular distance measured, as shown in Figure 7.

Since the objective of cluster analysis is to determine the representative structures of the conformational space explored, a carefully selected cut-off value is important as this method will avoid choosing subclusters. Accordingly the RMSD value of 0.8 Å was chosen as a cut-off value. Since another goal of this work was to get a better understanding of the structural motifs of the NMB peptide, further conformational analysis for this peptide was carried out

on the low energy structures. The 205 unique conformations were thereby classified into ten clusters (D1 to D10), summarized in Table 2. For each of the ten different classes of clusters, a representative of the cluster was chosen on the basis of having the lowest relative energy (designated by  $E_r$  min, Table 2).

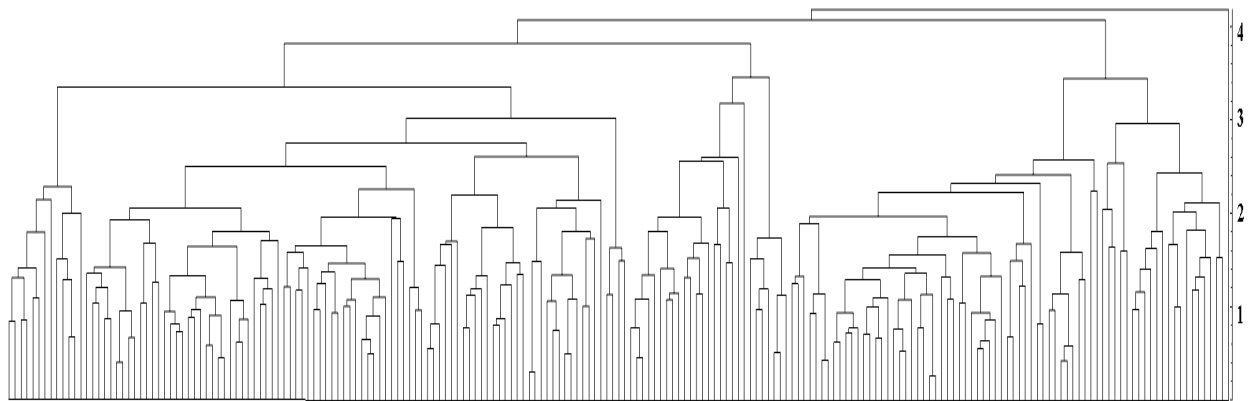


Fig. 7. Dendrogram showing different clusters for NMB classified according to their RMSD (shown along y-axis) using the Kleiweg clustering method.

Cluster name	percentage of structures in the cluster	Structure representative of the cluster	$E_r$ min /Kcal mol <sup>-1</sup>
D1	0.5	39	4.2
D2	10.2	142	3.9
D3	3.4	140	2.8
D4	41.6	108	4.7
D5	0.5	201	3.8
D6	21.9	87	1.5
D7	6.3	110	2.9
D8	9.2	116	1.9
D9	3.9	193	4.0
D10	2.4	123	4.4

Table 2. Cluster analysis for H-GNLWATGHFM-NH<sub>2</sub>.

The five most abundant clusters represented by D2, D4, D6, D7 and D8 in Table 2 corresponds to 10.2%, 41.6%, 21.9%, 6.3% and 9.2% of the total number of structures respectively, clearly suggesting that the bulk of the structures are restricted to small number of clusters. Inspection of Table 2 reveals that 89% of the structures are represented by the most abundant clusters.

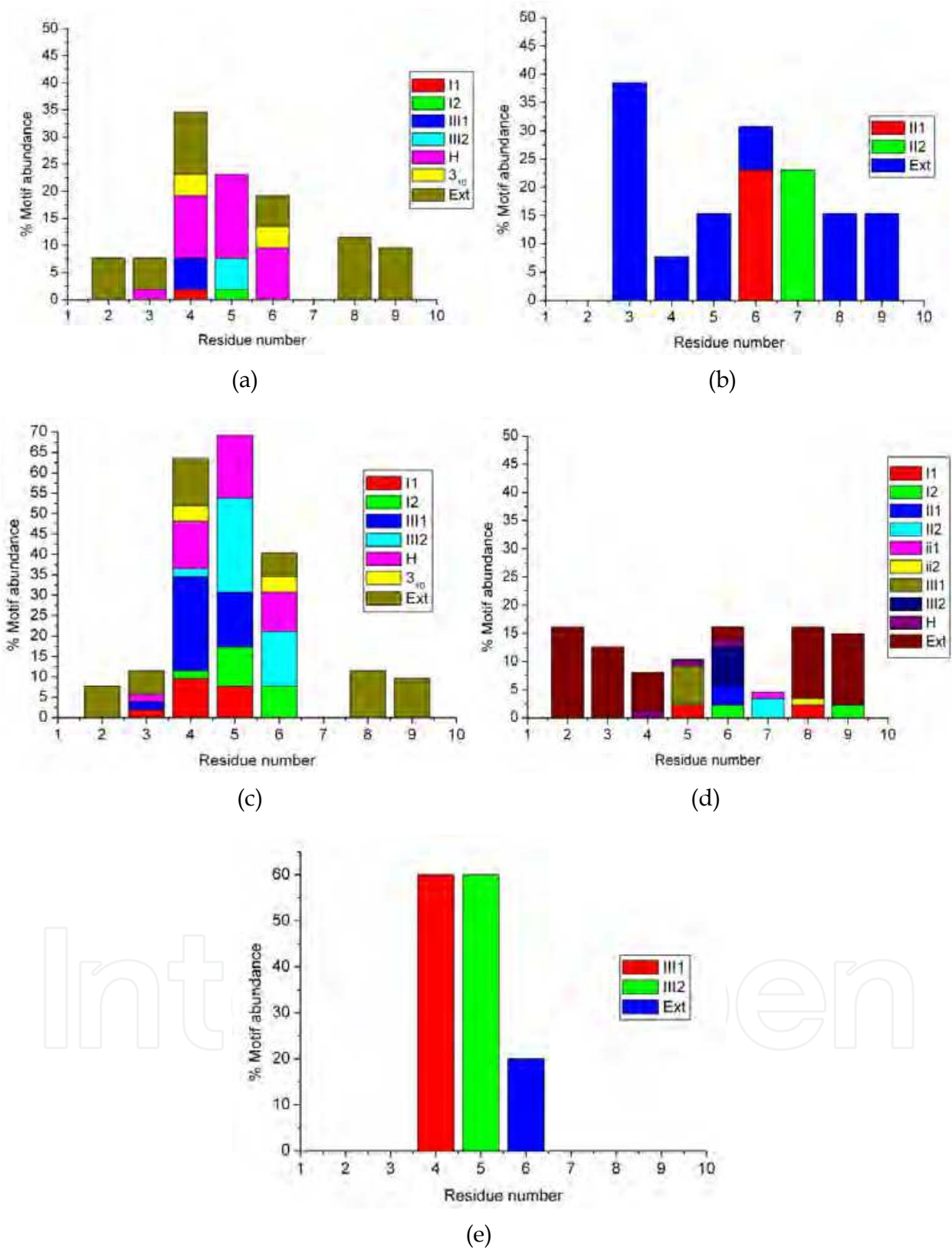


Fig. 8. Conformational motif abundance attained by NMB peptides in (a) cluster D2 (b) cluster D4 (c) cluster D6 (d) cluster D7 and (e) cluster D8. Conformational motifs are labeled: H ( $\alpha$ -helix),  $3_{10}$  ( $3_{10}$ -helix) and Ext (extended).



All the structures in each of the five most abundant clusters were analyzed to determine the conformational motifs attained by the NMB peptide, using CLASTERIT algorithm of the CLASICO program (Corcho, 2004).

The statistics of all the motifs found in clusters D2, D4, D6, D7 and D8 are depicted in Figures 8a–8e respectively. A closer inspection of Figure 8a reveals that most of the structures in cluster D2 (Table 2) predominantly exhibit an  $\alpha$ -helical region between residues 3 to 6, while most of the residues (2-4, 8-9, Figure 8a) prefer to stay in the extended form. The structures of the most populated cluster D4, on other hand, were observed displaying a  $\beta$ -turn type II between residues 6 and 7 while the rest showed only an extended region (Figure 8b). The conformations of the second most abundant cluster D6 (Figure 8c) displayed predominantly an  $\alpha$ -helical region between residues 3 to 6 with a stronger propensity between residues 4-5. To some extent the  $\beta$ -turn type III ( $3_{10}$ - $\alpha$  helical) and type I between residues 3-6 were also observed in some of the structures. However residue 7 did not show any secondary structural feature as most of the structures in clusters D7 were extended, while some displaying  $\alpha$ -helical region between residues 4-6 and  $\beta$ -turns of type II and type I between residues 6-7 and 5-6 respectively, were also part of the cluster (Figure 8d). Almost 60 % of the structures in cluster D5 did not display any ordered conformation except a  $\beta$ -turn type III ( $3_{10}$ - $\alpha$  helical) between residues 4 and 5 (Figure 8e).

#### 4. Conclusion

The present results suggest that the peptide adopts different folded and unfolded conformations regardless of the protocols used. REMD under GB conditions sample the new patterns in a uniform fashion and appears to have easily reached the convergence (Figure 6.3b), whereas conformations within the MD simulation seems to get trapped in certain regions of the conformational space making it less efficient. Moreover, the results obtained from REMD and MD computational protocols were compared with the available NMR results of NMB in literature. The comparison indicates that REMD shows good agreement with the reported NMR results. MD results, on the other hand, do not correspond with the reported NMR NOEs, clearly indicating the absence of NMR derived structures in this simulation. Moreover, the results obtained from SA is also in agreement with the corresponding REMD results clearly suggesting the probable existence of both turns and helicity in the NMB peptide, and thus may be responsible for binding of NMB at its receptor site. Hence, the present work provides comprehensive information about the conformational preferences of NMB explored using three different techniques which could be helpful to better understand its native conformation for future investigations.

#### 5. Acknowledgement

Dr P Singh gratefully acknowledges the financial support from the Durban University of Technology, and the National Research Foundation (NRF). KB gratefully acknowledges the experiences and insights gained from the Spanish collaborators through the SA-Spain bilateral agreement. The authors would like to express their acknowledgement to the Centre for High Performance Computing, an initiative supported by the Department of Science and Technology of South Africa.

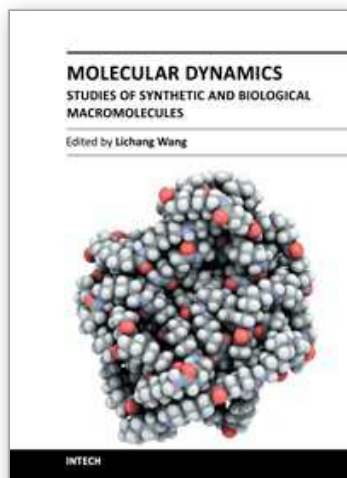
## 6. References

- Minamino, N.; Kangawa, K. & Matsuo, H. (1983). Neuromedin B: a novel bombesin like peptide identified in porcine spinal cord, *Biochemical and Biophysical Research Communications*, Vol.114, pp. 541-548.
- Erspamer, V. (1980). *Comprehensive Endocrinology* (Glass, G.B.J., Ed.). 343-361, Raven Press, New York.
- Marki, W.; Brown, M. & Rivier, J. E. (1981). Bombesin analogs: Effects on thermoregulation and glucose metabolism, *Peptides Supplement*, Vol.2, pp. 169-177.
- Ghatei, M. A.; Jung, R. T.; Stevenson, J. C.; Hillyard, C. J.; Adrian, T. E.; Lee, Y. C.; Christofides, N. D.; Sarson, D. L.; Mashiter, K.; MacIntyre, I. & Bloom, S.R. (1982). Bombesin - Action on gut hormones and calcium in man, *The Journal of Clinical Endocrinology and Metabolism*, Vol.54, pp. 980-985.
- Erspamer, V. (1988). Discovery, isolation and characterization of bombesin-like peptides, *Annals of the New York Academy of Science*, Vol.547, pp. 3-9.
- Cuttitta, F.; Carney, D. N.; Mulshine, J.; Moody, T. W.; Fedorko, J.; Fischler, A. & Minna, J. D. (1985). Bombesin-like peptides can function as autocrine growth factors in human small-cell lung cancer, *Nature*, Vol.316, pp. 823-826.
- Corps, A. N.; Rees, L. H. & Brown, K. D. (1985). A peptide that inhibits the mitogenic stimulation of Swiss 3T3 cells by bombesin or vasopressin, *Biochemical Journal*, Vol.231, pp. 781-784.
- Moody, T. W.; Carney, D. N.; Cuttita, F.; Quattrocchi, K. & Minna, J. D. (1985). High affinity receptors for bombesin/GRP-like peptides on human small cell lung cancer, *Life Sciences*, Vol.37, pp. 105-113.
- Ohki-Hamazaki, H. (2000). Neuromedin B, *Progress in Neurobiology*, Vol.62, pp. 297-312.
- Wada, E.; Way, J.; Shapira, H.; Kusano, K.; Lebacqz-Verheyden, A. M.; Coy, D.; Jensen, R. & Battey, J. (1991). cDNA cloning, characterization, and brain region-specific expression of a neuromedin-B-preferring bombesin receptor, *Neuron*, Vol.6, pp. 421-430.
- Corjay, M. H.; Dobrzanski, D. J.; Way, J. M.; Viallet, J.; Shapira, H.; Worland, P.; Sausville, E. A. & Battey, J. F. J. (1991). Two distinct bombesin receptor subtypes are expressed and functional in human lung carcinoma cells, *Journal of Biological Chemistry*, Vol.266, pp. 18771-18779.
- Gorbulev, V.; Akhundova, A.; Biichner, H. & Fahrenholz, F. (1992). Molecular cloning of a new bombesin receptor subtype expressed in uterus during pregnancy, *European Journal of Biochemistry*, Vol.208, pp. 405-410.
- Mantey, S.; Weber, C.; Sainz, E.; Akeson, M.; Ryan, R.; Pradhan, T.; Searles, R.; Spindel, E.; Battey, J. F.; Coy, D. H. & Jensen, R. T. (1997). Discovery of a high affinity radioligand for the human orphan receptor, bombesin receptor subtype 3, which demonstrates it has a unique pharmacology compared to other mammalian bombesin receptors, *The Journal of Biological Chemistry*, Vol.272, pp. 26062-26071.
- Lee, S. & Kim, Y. (1999). Solution structure of neuromedin B by <sup>1</sup>H nuclear magnetic resonance spectroscopy, *FEBS letters*, Vol.460, pp. 263-269.
- Erneand, D. & Schwyzer, R. (1987). Membrane structure of bombesin studied by infrared spectroscopy. Prediction of membrane interactions of gastrin-releasing peptide, neuromedin B, and neuromedin C, *Biochemistry*, Vol.26, pp. 6316-6319.

- Polverini, E.; Casadio, R.; Neyroz, P. & Masotti, L. (1998). Conformational changes of Neuromedin B and Delta sleep inducing peptide induced by their interaction with lipid membranes as revealed by spectroscopic techniques and molecular dynamics simulations, *Archives of Biochemistry and Biophysics*, Vol.349, pp. 225-235.
- Horwell, D.C.; Howson, W.; Naylor, D.; Osborne, S.; Pinnock, R. D.; Ratclii, G. S. & Suman-Chauman, N. (1996). Alanine scan and N-methyl amide derivatives of Ac-bombesin[7-14]. Development of a proposed binding conformation at the neuromedin B (NMB) and gastrin releasing peptide (GRP) receptors, *International Journal of Peptide and Protein Research*, Vol.48, pp. 522-531.
- Sainz, E.; Akeson, M.; Mantey, S. A.; Jensen, R. T. & and Battey, J. F. (1998). Four Amino Acid Residues Are Critical for High Affinity Binding of Neuromedin B to the Neuromedin B Receptor, *Journal of Biological Chemistry*, Vol.273, pp. 15927-15932.
- Erne, D.; Sargent, D. F. & Schwyzer, R. (1985). Preferred conformation, orientation and accumulation of dynorphin A(1-13), *Biochemistry*, Vol.24, pp. 4261-4263.
- Kaiser, E. T. & Kezdy, F. J. (1987). Peptides with affinity for membranes, *Annual Review of Biophysics and Biophysical Chemistry*, Vol.16, pp. 561-581.
- Dyson, H. J. & Wright, P. E. (1991). Peptide conformation and protein folding, *Annual Review of Biophysics and Biophysical Chemistry*, Vol.20, pp. 519-538.
- Zhong, L. & Jr. Johnson, W. C. (1992). Environment Affects Amino Acid Preference for Secondary Structure, *Proceedings of the National Academy of Sciences USA*, Vol.89, pp. 4462-4465.
- Coy, D. H.; Heinz-Erian, P.; Jiang, N.-Y.; Sasaki, Y.; Taylor, J.; Moureau, J.-P.; Wolfrey, W. T.; Gardner, J. D. & Jensen, R. T. (1988). Probing peptide backbone function in bombesin: a reduced peptide bond analogue with potent and specific receptor antagonist activity, *Journal of Biological Chemistry*, Vol.263, pp. 5056-5060.
- Rivier, J. E. & Brown, M. R. (1978). Bombesin, bombesin analogs, and related peptides: Effects on thermoregulation, *Biochemistry*, Vol.17, pp.1766-1771.
- Schwyzzer, R. (1986). Molecular mechanism of opioid receptor selection, *Biochemistry*, Vol.25, pp. 6335-6342.
- Dominy, B. & Brooks, C. (1999). Development of a Generalized Born Model Parameterization for Proteins and Nucleic Acids, *Journal of Physical Chemistry B*, Vol.103, pp. 3765-3773.
- Calimet, N.; Schaefer, M. & Simonson, T. (2001). Continuum solvent molecular dynamics study of flexibility in interleukin-8, *Journal of Molecular Graphics and Modelling*, Vol.19, pp. 136-145.
- Feig, M.; Im, W. & Brooks 3rd, C. L. (2004). Implicit Solvation Based on Generalized Born Theory in Different Dielectric Environment, *Journal of Chemical Physics*, Vol.120, pp. 903-911.
- Sigalov, G.; Scheffel, P.; Onufriev, A. (2005). Incorporating variable dielectric environments into the generalized Born model, *Journal of Chemical Physics*, Vol.122, pp. 094511-094515.
- Onufriev, A.; Bashford, D. & Case, D. A. (2004). Exploring protein native states and large-scale conformational changes with a modified generalized born model, *Proteins: Structure, Function, and Bioinformatics*, Vol.55, pp. 383-394.
- Terada, T. & Shimizu, K. (2008). A comparison of generalized Born methods in folding simulations, *Chemical Physics Letters*, Vol.460, pp. 295-299.

- Case, D. A.; Darden, T. A.; Cheatham, T. E. III.; Simmerling, C. L.; Wang, J.; Duke, R. E.; Luo, R.; Merz, K. M.; Pearlman, D. A.; Crowley, M.; Walker, R. C.; Zhang, W.; Wang, B.; Hayik, S.; Roitberg, A.; Seabra, G.; Wong, K. F.; Paesani, F.; Wu, X.; Brozell, S.; Tsui, V.; Gohlke, H.; Yang, L.; Tan, C.; Mongan, J.; Hornak, V.; Cui, G.; Beroza, P.; Mathews, D. H.; Schafmeister, C.; Ross, W. S. & Kollman, P. A. (2006). AMBER 9. University of California, San Francisco.
- Sitkoff, D.; Sharp, K. A. & Honig, B. (1994). Accurate Calculation of Hydration Free Energies Using Macroscopic Solvent Models, *Journal of Physical Chemistry*, Vol.98, pp.1978-1988.
- Tsui, V. & Case, D. A. (2001). Theory and applications of the generalized Born solvation model in macromolecular simulation, *Biopolymers*, Vol.56, pp.275-291.
- Wu, X. & Brooks, B. R. (2003). Self-guided Langevin dynamics simulation method, *Chemical Physics Letters*, Vol.381, pp. 512-518.
- Andersen, H. C. (1980). Molecular dynamics simulations at constant pressure and/or temperature, *Journal of Chemical Physics*, Vol.72, pp. 2384-2393.
- Ghose, A. K.; Crippen, G. M.; Revankar, G. R.; Smee, D. F.; McKernan, P. A. & Robins, R. K. (1989). Analysis of the in Vitro Antiviral Activity of Certain Ribonucleosides against Parainfluenza Virus Using a Novel Computer Aided Receptor Modeling Procedure, *Journal of Medicinal Chemistry*, Vol.32, pp. 746-756.
- Jörgensen, W. L. (1991). Rusting of the lock and key model for protein-ligand binding, *Science*, Vol.254, pp. 954-955.
- Corcho, F. J.; Filizola, M. & Perez, J. J. (1999). Assessment of the bioactive conformation of the farnesyltransferase protein binding recognition motif by computational methods, *Journal of Biomolecular Structure & Dynamics*, Vol.5, pp. 1043-1052.
- LaFargaCPL: CLASTERIT: Project Info. Available at:  
<https://lafarga.cpl.upc.edu/projects/clusterit> [Accessed June 12, 2008].
- Corcho, F.; Canto, J. & Perez, J. J. (2004). Comparative analysis of the conformational profile of substance P using simulated annealing and molecular dynamics, *Journal of Computational Chemistry*, Vol.25, pp.1937-1952.
- Filizola, M.; Centeno, N. B.; Farina, M. C. & Perez, J. J. (1998). Conformational analysis of the highly potent bradykinin antagonist Hoe-140 by means of two different computational methods, *Journal of Biomolecular Structure & Dynamics*, Vol.15, pp. 639-652.
- Kleiweg, P.; Nerbonne, J. & Bosveld, L. (2004). Geographical Projection of cluster composites. In: A. Blackwell, K. Marriott and A. Shimojima (Eds.).
- Jain, A. K.; Murty, M. N. & Flynn, P. J. (1999). Data Clustering: A Review. *ACM Computing Surveys* Vol.31, No.3. pp. 264-323.





## **Molecular Dynamics - Studies of Synthetic and Biological Macromolecules**

Edited by Prof. Lichang Wang

ISBN 978-953-51-0444-5

Hard cover, 432 pages

**Publisher** InTech

**Published online** 11, April, 2012

**Published in print edition** April, 2012

Molecular Dynamics is a two-volume compendium of the ever-growing applications of molecular dynamics simulations to solve a wider range of scientific and engineering challenges. The contents illustrate the rapid progress on molecular dynamics simulations in many fields of science and technology, such as nanotechnology, energy research, and biology, due to the advances of new dynamics theories and the extraordinary power of today's computers. This second book begins with an introduction of molecular dynamics simulations to macromolecules and then illustrates the computer experiments using molecular dynamics simulations in the studies of synthetic and biological macromolecules, plasmas, and nanomachines. Coverage of this book includes: Complex formation and dynamics of polymers Dynamics of lipid bilayers, peptides, DNA, RNA, and proteins Complex liquids and plasmas Dynamics of molecules on surfaces Nanofluidics and nanomachines

### **How to reference**

In order to correctly reference this scholarly work, feel free to copy and paste the following:

Parul Sharma, Parvesh Singh, Krishna Bisetty and Juan J Perez (2012). An Assessment of the Conformational Profile of Neuromedin B Using Different Computational Sampling Procedures, *Molecular Dynamics - Studies of Synthetic and Biological Macromolecules*, Prof. Lichang Wang (Ed.), ISBN: 978-953-51-0444-5, InTech, Available from: <http://www.intechopen.com/books/molecular-dynamics-studies-of-synthetic-and-biological-macromolecules/an-assessment-of-the-conformational-profile-of-neuromedin-b-using-different-computational-sampling-p>

**INTech**  
open science | open minds

### **InTech Europe**

University Campus STeP Ri  
Slavka Krautzeka 83/A  
51000 Rijeka, Croatia  
Phone: +385 (51) 770 447  
Fax: +385 (51) 686 166  
[www.intechopen.com](http://www.intechopen.com)

### **InTech China**

Unit 405, Office Block, Hotel Equatorial Shanghai  
No.65, Yan An Road (West), Shanghai, 200040, China  
中国上海市延安西路65号上海国际贵都大饭店办公楼405单元  
Phone: +86-21-62489820  
Fax: +86-21-62489821



© 2012 The Author(s). Licensee IntechOpen. This is an open access article distributed under the terms of the [Creative Commons Attribution 3.0 License](https://creativecommons.org/licenses/by/3.0/), which permits unrestricted use, distribution, and reproduction in any medium, provided the original work is properly cited.

IntechOpen

IntechOpen